

## Using Sodium Caseinate and Balango Gum Complex to Produce Crocin Nanoemulsion and Investigate Its Qualitative Characteristics and Release in Model Systems

Roghayeh Ezzati<sup>1</sup>, Leila Roozbeh Nasiraei<sup>1\*</sup>, Sara Jafarian<sup>1</sup>, Masoud Dezyani<sup>2</sup>, Fatemeh Shahdadi<sup>3</sup>

<sup>1</sup>Department of Food Science, Nour Branch, Islamic Azad University, Nour, Iran

<sup>2</sup>Department of Food Science, Gorgan Branch, Islamic Azad University, Gorgan, Iran

<sup>3</sup>Department of Food Science, Faculty of Agriculture, University of Jiroft, Jiroft, Iran

\*Corresponding Author: Roozbeh Nasiraei, Department of Food Science, Nour Branch, Islamic Azad University, Nour, Iran, E-mail: leylaroozbehnasiri@gmail.com

Received Date: May 05, 2026 Accepted Date: June 05, 2026 Published Date: June 08, 2026

Citation: Roghayeh Ezzati, Leila Roozbeh Nasiraei, Sara Jafarian, Masoud Dezyani, Fatemeh Shahdadi (2026) Using Sodium Caseinate and Balango Gum Complex to Produce Crocin Nanoemulsion and Investigate Its Qualitative Characteristics and Release in Model Systems. J Nanotech Smart Mater 12: 1-29

### Abstract

Crocins are water-soluble carotenoids and bioactive color compounds of saffron. This pigment is unstable to various environmental conditions such as temperature, light, oxygen and the presence of metal ions. Encapsulation aims to prevent the degradation of these compounds by environmental factors, degradation in the human digestive tract and provide controlled release of the compounds and thus improve bioavailability. The aim of this study is to use sodium caseinate and balango gum complex to produce nanoemulsion (encapsulated crocin) and investigate its qualitative characteristics and release in model systems. The complex prepared from balango and sodium caseinate (0.5:0.5%) was used as a wall and emulsifier (0.25, 0.5 and 1%) to produce nanoencapsulated crocin, and then under pressure of 300 and 500 bar, properties such as particle size, stability and efficiency were investigated. The results showed that the sample containing 1% emulsifier and the complex of sodium caseinate and balango gum at a pressure of 500 bar obtained better results. To dry the nanoemulsion (crocin microencapsulated by balango gum and sodium caseinate), a spray dryer was used with inlet air temperatures of 150, 170 and 190°C and inlet feed temperatures of 60, 70 and 80°C. The highest efficiency and best physical properties were obtained at an air temperature of 190 and a feed temperature of 60°C. The optimized dried nanoemulsion powders were investigated in terms of their release rate in the stomach and intestines condition and release modeling in 15% sucrose solution at pH 4, 6, and 8, temperatures of 5, 50, and 75°C, and durations of 30, 60, 90, 120, 150, and 180 min. The release of nanoencapsulated crocin was a function of pH, temperature and time and under low pH, high temperature and time, the re-

lease rate increased. The modeling results in 15% sucrose solution showed that at different pH and temperatures, the Peppas, Higuchi, and first-order models were fit, and in modeling the release in the stomach and intestine, the Peppas model was also fit. Finally, the results showed that the wall materials used for encapsulating crocin made it stable in the stomach simulation stage and its sustained release.

**Keywords:** Nanoencapsulation; Crocin; Release; Spray Drying

## Introduction

Saffron has many applications in the production of food, pharmaceutical and chemical products due to its excellent taste and color, and is considered an expensive product due to the limitations of cultivation and production. Saffron is also used in the treatment of some cancers, cerebrovascular and cardiovascular diseases, diarrhea, measles, genital infections, asthma and gastrointestinal disorders. A large part of the therapeutic properties of saffron are attributed to crocin (responsible for the red color of saffron) and its analogues, and it seems that this property of crocin is due to its sugar part (Chen et al., 2008). Given that crocin is sensitive to changes in pH, temperature, and light, which limits the color stability of saffron-containing products, microencapsulation techniques are used to stabilize the color of saffron. The protection and control of the release of active compounds such as crocin, picrocrocin, and safranal leads to increased efficacy. Nano/microencapsulation techniques for poorly water-soluble biological compounds have received much attention for maintaining their biological activity and controlled release (Agustin and Hammar, 2009; Mozaffari et al., 2009). Microencapsulation is a method in which a solid, liquid, or gas compound is placed in small capsules and released under specific conditions (Azilassi et al., 2013). This technology is used in the food industry for various reasons, including: protecting the core compound from degradation by external environmental factors, reducing the evaporation or transfer rate of the core compound to the outside environment, releasing the core slowly over time or at a specific time, and ... (Desai and Park, 2005).

Tapal and Tiko (2012) studied the solubility and stability of crocin and soy protein isolate complexes. Fluorescence spectroscopy showed that the complex formation occurs through hydrophobic interactions, and ultraviolet spectroscopy showed that more than 80% of the complexed

crocin was stable in simulated gastric and intestinal fluids for 12 hours.

Pen et al. (2013) investigated the enhancement of bioactivity and dispersibility of curcumin by encapsulation in casein nanocapsules by spray drying. The results showed no crystallization, improved thermal stability, and increased solubility (4-fold) of curcumin.

Finding new cheap, accessible, and effective compounds in encapsulation of compounds and creating functional food compounds can be a way to achieve healthier nutrition and ultimately ensure the health of the community. The use of new wall compounds (sodium caseinate-balangu seed gum complex) that, in addition to affecting product characteristics, have functional, cheap, and available properties, will be considered in this research. Granular mucilages and plant polysaccharides are in this category. Balangu, (*Lallemantia royleana*), is a glazed plant from the mint family that grows in different regions of the world, especially in the Middle East. Balangu seeds are elongated oval in shape and can be cultivated and harvested in Asia and Northern Europe, and in Iran they are generally referred to as syrup seeds. If Balangu seeds are soaked in water, they produce a viscous, turbid, and tasteless liquid (mucilage). Due to the production of high amounts of mucilage, this seed can be used as a new source of hydrocolloid in the food industry for various purposes (Zamani et al. 2015; Salehi 2020). Balango seed gum contains 61.74% carbohydrates, 0.87% protein, 29% crude fiber, and 33.8% ash (Salehi et al., 2014). Sodium caseinate is the sodium salt of casein, which has a pleasant taste and can easily form aqueous solutions due to its ability to form extensive intermolecular hydrogen bonds. It is highly soluble and disperses very quickly in an aqueous mixture and is also homogenized in the presence of oil and fat. Casein coatings and films are used as a microencapsulating agent for flavors, drugs, and coatings for fruits, vegeta-

bles and cheese (Khaldia et al., 2011). Sodium caseinate can easily form a film from an aqueous solution. This material is effective in film formation due to its casein structure and amino acid sequence, hydrogen bonds, electrostatic interactions, and hydrophobic forces (Atares et al., 2010).

Although studies have been conducted on complexing crocin with proteins, the use of protein-polysaccharide complexes (sodium caseinate-balango seed gum) for nanoencapsulation of crocin and investigation of its release kinetics in simulated models has received less attention. Therefore, the aim of this research is to use a new and cost-effective as the encapsulation wall of crocin pigment and to produce a stable nanoproduct powder with controlled release for use in the food and pharmaceutical industries.

## Materials and Methods

The chemicals used in this study were crocin in the form of digentiobiosecrocin ester (Sigma, USA), polyglycerol ricinoleate emulsifier (Palsgaard, Denmark), sodium caseinate (Sigma, New Zealand), sodium hydroxide (Merck, Germany), hydrochloric acid (Merck, Germany).

The balango seeds used in this study were purchased from stores in Tabriz and after grinding with (Sanyo, Japan) and passing through a sieve (mesh size of 60), the resulting powder was stored in zippered bags in a cool, dry place for experiments.

### Preparation of Nanocomplex of Balangu and Sodium Caseinate Containing Crocin Nanoemulsion

The desired amount of balango powder was added to distilled water and the mixture was stirred for 12 hours by a magnetic stirrer at 4000 rpm to absorb water and create a uniform texture. After heating for 10 min in a water bath (to help absorb water) at 70°C, it was stored at refrigerator (4°C) for 12 h to complete the water absorption process. Sodium caseinate powder was also added to distilled water and after 30 min of mixing by a magnetic stirrer, it was stored overnight at 4°C to ensure complete dissolution and dehydration (Qasemi et al., 2017). Sodium caseinate (0.5%) and balango solution (0.5%) were mixed together and after

adjusting the pH to 3.5 to prepare the nanocomplex (optimal pH for preparing the nanocomplex), the resulting mixture was passed through a high-pressure homogenizer.

Polyglycerol ricinoleate (HLB: 1.5) was used to prepare the water-in-oil emulsion. A 10% w/w solution of crocin was mixed with different concentrations of emulsifier (0.5, 1 and 1.5%) on a magnetic stirrer. The aqueous phase containing the emulsifier was added dropwise to the oil phase (corn oil). Then, the resulting emulsion was mixed at a constant speed of 1000 rpm for one hour. To prepare the bilayer emulsion, a 10% w/w water-in-oil microemulsion was added to the aqueous solution containing the sodium caseinate/balango seed gum complex (90% w/w). This mixture was processed for 5 min at 1000 rpm using a closed-loop ultratorque and then by a high-pressure homogenizer (2000 bar) (Tazari 2023).

### Drying of Balangu and Sodium Caseinate Nanocomplex Containing Crocin Nanoemulsion by Spray Method

A spray dryer was used to dry the emulsion liquid. The inlet air temperature (150, 170 and 190 °C) and the inlet feed temperature (60, 70 and 80 °C) were considered. The outlet air temperature was 90 °C, the air flow rate was 80 kg/h and the water evaporation rate was 6 kg/h and its effect on the particle size characteristics, bulk density, apparent density, porosity, solubility, moisture, water activity, microstructure as well as the microencapsulation efficiency and loading efficiency of the resulting powder were investigated (Mohammadi, 2009).

### Determination of Crocin Amount

A spectrophotometer was used at a wavelength of 450 nm to determine the crocin concentration and to draw the relevant standard curve.

To determine the standard curve of crocin absorption, 6 mg of crocin was dissolved in 100 ml of hexane, then 0.25, 0.5, 1, 2.5, 3 and 4 ml of the solution were removed and diluted with hexane to 15 ml, respectively, obtaining concentrations of 1 to 16 mg/l. Hexane was used as a control in the spectrophotometer (Ma et al., 2017).

## Stability against Ph

The pH of the prepared emulsions was adjusted to pH 4.5, 6.5 and 8.5 using sodium hydroxide and acid solutions, and after being placed in a test tube at room temperature for 24 hours, the stability and efficiency of microencapsulation were measured (Ozturk et al., 2014).

Thermal stability was investigated at two temperature conditions of 63°C for 30 min and 95°C for 10 min by measuring the microencapsulation efficiency and nanoemulsion stability (Li et al., 2014).

## Measurement of Microencapsulation Efficiency (Total and Surface Crocin)

$$Eq(1) \quad \text{Nanoencapsulation efficiency} = \frac{\text{total crocin} - \text{free crocin}}{\text{total crocin weight}} \times 100$$

## Bulk Density

Bulk density was measured by pouring the sample into a container with known dimensions (Jafari and Kashani, 2010).

$$Eq[2] \quad V_p = \frac{(M_{pt} - M_p) - (M_{pst} - M_{ps})}{\rho_t}$$

$M_{pt}$ : Weight of pycnometer and toluene,  $M_p$ : Weight of pycnometer,  $M_{pst}$ : Weight of pycnometer, sample

To determine surface crocin, total crocin and calculate the nanoencapsulation efficiency, 0.5 g of the sample (nanoencapsulated crocin before and after drying) was mixed with 20 ml of hexane and then filtered with Whatman filter paper (No. 41) and the absorbance of the filtered solution was measured at a wavelength of 450 nm.

To calculate total crocin, 0.5 g of the sample was thoroughly mixed with 20 ml of water, then 10 ml of hexane was added to it, and after 5 min of mixing, it was centrifuged (3500 rpm for 20 min). The upper phase was collected and reported for spectrophotometry at 450 nm as total crocin in the biopolymer complex. The nanoencapsulation efficiency was calculated using the equation 1 (Ghaseemi et al., 2017a,b).

## Apparent Density

Calculated by displacement method using pycnometer. Toluene volume ( $V_p$ ) was calculated using equation 2 and apparent density using equation 3 (Qasemi et al., 2017).

$$Eq[3] \quad \rho_a = \frac{M_{ps} - M_p}{V_p}$$

$M_p$ : Weight of pycnometer,  $M_{ps}$ : Weight of pycnometer and sample,  $\rho_a$ : Apparent density,  $V_p$ : Apparent density.

and toluene,  $M_{ps}$ : Weight of pycnometer and sample,  $\rho_t$ : Density of toluene.

## Porosity

Porosity is calculated from the equation 4:

$$Eq[4] \quad \varepsilon = 1 - \frac{\rho_b}{\rho_a}$$

$\rho_b$ : Bulk density,  $\rho_a$ : Apparent density,  $\varepsilon$ : Porosity.

## Humidity and pH

The humidity of the powders was measured using a digital hygrometer.

The pH was measured using a pH meter.

## Water Activity

The NOVASINA Thermocontanter device was used to measure water activity.

## Solubility

The method of Sarabandi and Sadeghi Mahonak (2016) was used to measure the solubility of the powder. 1 gram of powder was carefully added to 100 ml of distilled water under stirring conditions with a magnetic stirrer at 700 rpm for 4 min. The resulting solution was centrifuged

at  $\times 300$  g for 4 min. 25 ml of the above solution was transferred to a pre-weighed Petri dish and dried in an oven at 105°C for 5 h. The weight of the dried solid relative to the initial powder was used to determine the solubility in water in percentage.

## Modeling the Release Process

The release of crocin was investigated in a food model as well as a simulated stomach and intestine model systems. The release of crocin was evaluated at different temperatures (4 and 70°C for 2 min) and pHs (4, 6 and 8) in the model system (15% w/v sucrose-water solution). The results will be investigated using empirically defined release models including zero-order, first-order, Higuchi, Hixsoncrowell and the Peppas (equations of 5,6,7, 8 and 9, respectively) (Mohammadi, 2009).

$$Eq(5) \quad C = C_0 + K_0t(3 - 11) \quad Zero - order$$

C is the release rate at time t,  $C_0$  is the initial nutrient amount,  $K_0$  is the model constant rate, t time.

$$Eq(6) \quad -Kt = \ln\left(\frac{C}{C_0}\right) \quad First - order$$

C is the release rate at time t,  $C_0$  is the initial nutrient amount, K is the model constant rate, t time

$$Eq(7) \quad \frac{M_t}{M_\infty} = K_H t^{0.5} \quad Higuchi$$

where  $M_t$  and  $M_\infty$  are the amounts of crocin released at time t and infinity, respectively, and  $k_H$  is the Higuchi release constant.

$$Eq(8) \quad K_{HCT} = C_0^{1/3} - C_t^{1/3} \quad Hickson - Crowell$$

C is the release rate at time t,  $C_0$  is the initial nutrient amount,  $K_{HC}$  is the model constant rate, t time.

$$Eq(9) \quad K_{t_0} = \frac{C_t}{C_\infty} \quad Peppas$$

$C_t/C_\infty$  is the nutrient release at time t, K is the constant rate, n is the release index, t time.

## Statistical Analysis

This experiment was conducted in a completely randomized factorial design. Statistical analysis of the results was performed using SPSS 22 software and means were compared with Duncan's test at a confidence level of 95%.

## Results and Discussion

### Crocin Absorbance at 452 Nm

The absorbance of different concentrations of crocin at 452 nm is shown in Figure 1. According to the figure, it can be seen that the higher the amount and concentra-

tion of crocin in the sample or complex, the higher the absorbance and the higher the turbidity. Therefore, the absorbance and turbidity are higher in samples containing more crocin. The coefficient of determination (99.56%) showed that there is a high correlation between the concentration of crocin and the absorbance.

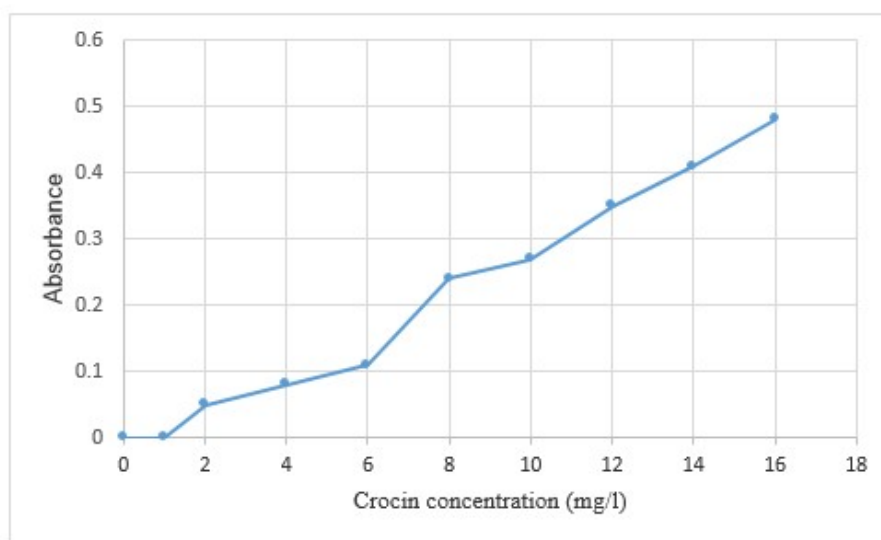


**Figure 1:** Crocin absorbance at 452 nm

**Table 1:** Effect of homogenization pressure and emulsifier concentration on the particle size (nm) of crocin nanoemulsion after 1 day

| Sample | 300 bar              | 500 bar              |
|--------|----------------------|----------------------|
| T1     | 1016.66 <sup>b</sup> | 1233.33 <sup>a</sup> |
| T2     | 914.33 <sup>bc</sup> | 856.66 <sup>d</sup>  |
| T3     | 713.33 <sup>c</sup>  | 570.00 <sup>f</sup>  |

T1: sample containing 0.25% emulsifier, T2: sample containing 0.5% emulsifier and T3: sample containing 1% emulsifier.

\*Different lowercase letters indicate significant differences ( $p \leq 0.05$ )

### Effect of Homogenization Pressure and Emulsifier Concentration on the Properties of Crocin Nanoemulsion

#### 1- Effect of homogenization pressure and emulsifier concentration on the droplet size of crocin nanoemulsion

Particle size and their distribution play an important role in the physical properties of colloidal systems such

as storage stability, turbidity and rheological properties, and also affect properties such as bioavailability, organoleptic and sensory properties of food products (Acosta, 2009). One of the important properties of nanoemulsions that affects the physicochemical properties such as rheological behavior and, consequently, the stability of these systems is the particle size distribution (PDI). Analysis of the data obtained from the particle size distribution provides appropriate information about the aggregation of emulsion particles

over time. Numerous studies have pointed out the reduction in droplet size due to the application of homogenization pressure. Increasing particle size leads to an increase in the oil-water interface in the emulsion, and therefore, to maintain stability, there must be sufficient emulsifier compounds to cover the newly created surfaces in the system, otherwise the droplets will reconnect and increase the dro-

plet size, causing instability (Kharat et al., 2018; Yone et al., 2017).

The effect of homogenization pressure and emulsifier concentration on the particle size of crocin nanoemulsion after 1 and 7 days is shown in Tables 1 and 2 and Figure 2.

**Table 2:** Effect of homogenization pressure and emulsifier concentration on the particle size (nm) of crocin nanoemulsion after 7 days

| Sample | 300 bar              | 500 bar               |
|--------|----------------------|-----------------------|
| T1     | 1316.66 <sup>b</sup> | 1586.66 <sup>a*</sup> |
| T2     | 900.00 <sup>c</sup>  | 843.33 <sup>d</sup>   |
| T3     | 696.66 <sup>e</sup>  | 580.00 <sup>f</sup>   |

T1: sample containing 0.25% emulsifier, T2: sample containing 0.5% emulsifier and T3: sample containing 1% emulsifier.

\*Different lowercase letters indicate significant differences ( $p \leq 0.05$ )

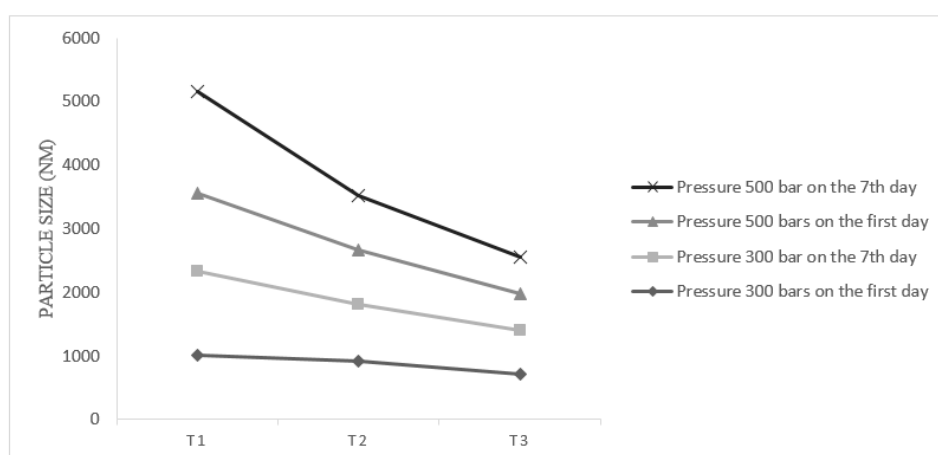


**Figure 2:** Effect of homogenization pressure and emulsifier concentration on particle size of crocin nanoemulsion

T1: sample containing 0.25% emulsifier, T2: sample containing 0.5% emulsifier and T3: sample containing 1% emulsifier

According to the data in Tables 1 and 2, there was a significant difference between the average particle size of nanocomplexes containing different amounts of emulsifier under homogenization pressure of 300 and 500 bar ( $p < 0.05$ ). The highest particle size after 1 and 7 days of production was for the sample containing 0.25% emulsifier under 500 bar and the lowest particle size was for the sample containing 1% emulsifier under 500 bar pressure. Except for the sample containing 0.25% emulsifier which has a higher particle size under 500 bar, in the other samples, the particle

size decreases with increasing homogenization pressure. Also, with increasing emulsifier content in the nanocomplex structure, the particle size decreases. According to Figure 2, the particle size of crocin nanocomplexes containing emulsifiers increases with the passage of time. The change in particle size with increasing homogenization pressure at a constant emulsifier concentration was dependent on the amount of emulsifier. At low emulsifier concentrations, the increase in droplet size can be related to the insufficient amount of emulsifier present in the medium to completely cover the

oil-water droplet interface, which caused the particles to connect to each other by various mechanisms such as aggregation and recalescence, followed by an increase in particle size and instability (Karadag et al., 2013; Harte and Venegas, 2010; Rocha-Jafari et al., 2008;). It is also possible that the droplets connect to each other through the phenomenon of aggregation due to bridge formation and, as a result, an increase in size. In this case, due to insufficient amount of emulsifier, one emulsifier molecule was adsorbed at the interface of several molecules, and as a result, the molecules were bound together, increasing the particle size (Wang et al., 2008). The decrease in particle size with increasing emulsifier concentration can be attributed to the presence of sufficient emulsifier to completely cover the newly formed surfaces. In this case, by creating a layer on the surface of the droplets due to the repulsive force created by spatial and electrostatic forces, the droplets were prevented from approaching each other and thus from connecting, and ultimately caused a decrease in particle size and stability (Fang and Bhesh, 2010).

In general, it can be said that increasing the homogenization pressure reduces the droplet size if the emulsifier is sufficient. In order to form an emulsion with a smaller particle size, more mechanical energy must be used, which in the high-pressure homogenization process can be identified by increasing the homogenization pressure or the number of cycles (Juttulapa et al., 2017). Jafari et al. (2008) also reported that the efficiency of the high-pressure homogenization process for reducing droplet size depends on the number of cycles and the homogenization pressure. Previous findings are also in agreement with the results of this study. In the study of Yong et al. (2017), the effect of homogenization pressure on the particle size of emulsion was also mentioned. They stated that the use of high pressure mechanically reduces the size of the globules to less than one micrometer and creates an emulsion with a uniform structure and higher stability. In general, the increase and decrease in particle size can be related to the intensification of interactions between polymers adsorbed at the water-oil interface with each other or with polymers that are freely present and move in the continuous phase. Under these conditions, droplet-droplet interactions and the possibility of network formation with the help of bridges or cluster formation increase. In general, various factors affect the particle

size of a nanoemulsion, including the type of phases, amount and type of emulsifier, nanoemulsion preparation methods, environmental conditions such as pH, the presence of metal ions, etc. (Jamshidi et al. 2020).

Ganji et al. (2020) used different percentages of gelatin for microencapsulation of crocin. According to their results, the size of encapsulated crocin particles increased significantly at higher gelatin concentrations, and smaller particle sizes were formed at lower gelatin concentrations. This can be attributed to the network created by the additional wall material and the increase in the wall thickness of the microcapsules (Taherian et al., 2006). Furthermore, in their study, PDI increased significantly with increasing gelatin concentration from 3% to 7%.

Nazari et al. (2023) studied the production of crocin nanoencapsulation using bilayer emulsions to increase the stability of this compound. According to the results, in the production of oil-in-water microemulsions, it was shown that with increasing the surfactant to oil phase ratio up to 100%, the droplet size decreased and then increased. At low speed, bilayer emulsions were not formed. In fact, there was no energy to separate the dispersed phase from the surfactant. The average particle size was about 11.40 nm at a speed of 500 rpm and when the speed was increased to 1000 rpm, the droplet size was 22.55 nm. The results also showed that, with increasing time, the average particle size increased from 9.32 to 45.04 and 53.06 nm. Another study found that if the oil/surfactant mixture is rapidly added to the aqueous phase in the production of oil-in-water microemulsions, viscous oil/surfactant/water aggregates spontaneously form (Yang et al., 2012).

#### **Effect of homogenization pressure and emulsifier concentration on the stability of crocin nanoemulsion**

Several factors such as oil type, surfactant type, emulsion composition, preparation method, mechanical pressure, droplet size, temperature, pH and ionic strength affect the stability of the emulsion (McClements, 2015). The emulsifiers used actually play the role of a wall in the nanoencapsulation process.

The effect of homogenization pressure and emulsifier concentration on the stability of crocin nanoemulsion

after 1 and 7 days is given in Tables 3 and 4 and Figure 3.

**Table 3:** Effect of homogenization pressure and emulsifier concentration on the stability (%) of crocin nanoemulsion after 1 day

| Sample | 300 bar            | 500 bar             |
|--------|--------------------|---------------------|
| T1     | 99.00 <sup>a</sup> | 84.00 <sup>b*</sup> |
| T2     | 98.33 <sup>a</sup> | 98.00 <sup>a</sup>  |
| T3     | 97.66 <sup>a</sup> | 99.00 <sup>a</sup>  |

T1: sample containing 0.25% emulsifier, T2: sample containing 0.5% emulsifier and T3: sample containing 1% emulsifier.

\*Different lowercase letters indicate significant differences ( $p \leq 0.05$ )

**Table 4:** Effect of homogenization pressure and emulsifier concentration on the stability (%) of crocin nanoemulsion after 7 days

| Sample | 300 bar            | 500 bar             |
|--------|--------------------|---------------------|
| T1     | 82.33 <sup>b</sup> | 75.66 <sup>c*</sup> |
| T2     | 97.66 <sup>a</sup> | 97.33 <sup>a</sup>  |
| T3     | 99.33 <sup>a</sup> | 98.33 <sup>a</sup>  |

T1: sample containing 0.25% emulsifier, T2: sample containing 0.5% emulsifier and T3: sample containing 1% emulsifier.

\*Different lowercase letters indicate significant differences ( $p \leq 0.05$ )

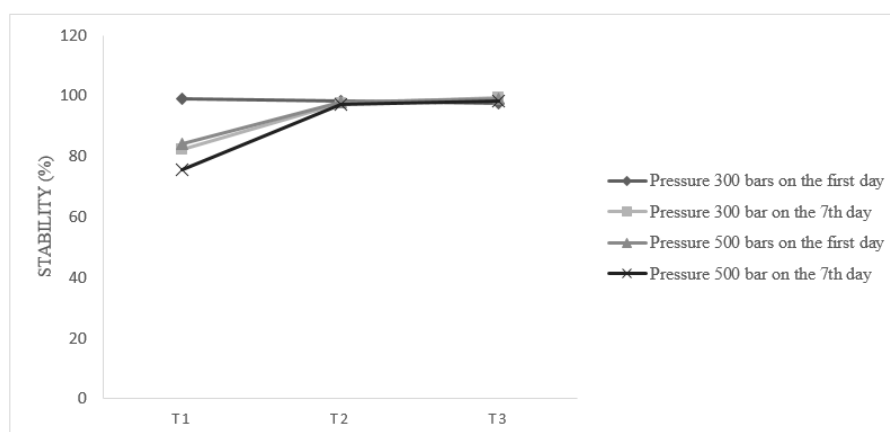


**Figure 3:** Effect of homogenization pressure and emulsifier concentration on stability of crocin nanoemulsion

T1: sample containing 0.25% emulsifier, T2: sample containing 0.5% emulsifier and T3: sample containing 1% emulsifier

The results of Tables 3 and 4 show that at 300 and 500 bar pressure on the first day of storage, there was no difference between the stability of nanoemulsion samples containing different amounts of emulsifier ( $p > 0.05$ ). On the seventh day of storage, this difference was significant only in the sample containing 0.25% emulsifier at 500 bar pressure

with the others ( $p < 0.05$ ). The nanoemulsion sample containing 0.25% emulsifier had a lower stability than the other samples. According to Figure 3, the stability of nanoemulsions on the 7th day of storage was lower than on the first day. With an increase in the amount of emulsifier in the structure of nanoemulsions, the stability increased.

In general, gums are hydrophilic molecules whose presence increases the continuous water space around the dispersed phase droplets and by stabilizing this space in a gel-like network by creating steric hindrance, they reduce the rate of creaming and ultimately increase the stability of the emulsion (Tariqati et al., 1401). As a result, since balan-go gum is used in the structure of the microencapsulated nanoemulsion, and with increasing the amount of emulsifier, the amount of gum in the formulation increases, so the stability increases. Some studies have shown that the decrease in emulsion particle size, which generally indicates an increase in emulsion stability, results in greater retention of active ingredients (Dehghan et al. 2018).

The viscosity of emulsions plays an important role in the stability of emulsions, and with increasing viscosity, the movement of dispersed phase droplets towards each other decreases and the aggregation of droplets is prevented. The viscosity of all microcapsules increases with increasing surfactant content. This increase in viscosity can be due to the increase in free surfactant in the continuous phase,

which leads to an increase in emulsion viscosity (An et al., 2014).

### 3- Effect of homogenization pressure and emulsifier concentration on the efficiency of crocin nanoemulsion

One of the first characteristics considered in the microencapsulation process is the determination of the microencapsulation efficiency to determine the effectiveness of the process used to prepare the coatings. In fact, the nanoencapsulation efficiency indicates how much of the initial crocin used is loaded into the nanoencapsulations. Since one of the characteristics of gums is their adhesive property, it is expected that the crocin trapped inside the nanoencapsulation and the crocin bound to the surface, both of which are considered as the microencapsulation efficiency (Tariqati et al., 1401).

The effect of homogenization pressure and emulsifier concentration on the efficiency of crocin nanoemulsion after 1 and 7 days is shown in Tables 5 and 6 and Figure 4.

**Table 5:** Effect of homogenization pressure and emulsifier concentration on the efficiency (%) of crocin nanoemulsion after 1 day

| Sample | 300 bar pressure   | 500 bar pressure    |
|--------|--------------------|---------------------|
| T1     | 37.66 <sup>d</sup> | 29.00 <sup>e'</sup> |
| T2     | 55.33 <sup>c</sup> | 62.66 <sup>b</sup>  |
| T3     | 61.33 <sup>b</sup> | 71.00 <sup>a</sup>  |

T1: sample containing 0.25% emulsifier, T2: sample containing 0.5% emulsifier and T3: sample containing 1% emulsifier.

\*Different lowercase letters indicate significant differences ( $p \leq 0.05$ )

**Table 6:** Effect of homogenization pressure and emulsifier concentration on the efficiency (%) of crocin nanoemulsion after 7 days

| Sample | 300 bar pressure    | 500 bar pressure    |
|--------|---------------------|---------------------|
| T1     | 32.33 <sup>e</sup>  | 26.66 <sup>f'</sup> |
| T2     | 57.00 <sup>d</sup>  | 62.33 <sup>bc</sup> |
| T3     | 66.33 <sup>ab</sup> | 70.33 <sup>a</sup>  |

T1: sample containing 0.25% emulsifier, T2: sample containing 0.5% emulsifier and T3: sample containing 1% emulsifier.

\*Different lowercase letters indicate significant differences ( $p \leq 0.05$ )

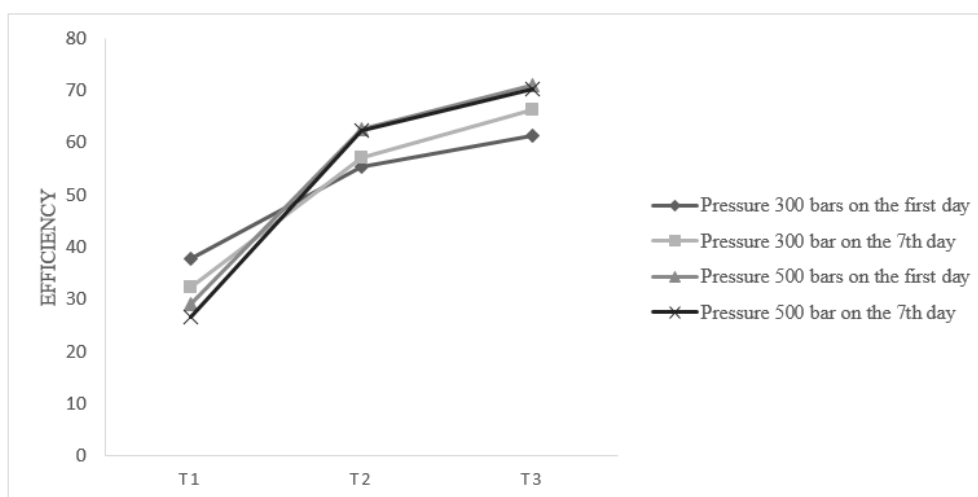


**Figure 4:** Effect of homogenization pressure and emulsifier concentration on efficiency of crocin nanoemulsion

T1: sample containing 0.25% emulsifier, T2: sample containing 0.5% emulsifier and T3: sample containing 1% emulsifier

According to the results of Tables 5 and 6, on the first day, there was a difference in the efficiency of the encapsulated nanoemulsion samples ( $p < 0.05$ ), and the nanoencapsulated nanoemulsion sample containing 1% emulsifier under a pressure of 500 bar had the highest efficiency. On the 7th day, the lowest efficiency was observed in the sample containing 0.25% emulsifier under a pressure of 500 bar, and the microencapsulated nanoemulsion sample containing 1% emulsifier under a homogenization pressure of 500 bar had the highest efficiency. The efficiency of nanoencapsulation was higher at higher pressures, which may be due to the availability of more functional groups due to the increase in surface area or the change in the spatial structure of these materials to create different bonds. Increasing the homogenization pressure by reducing the particle size and rearranging the biopolymers increased the possibility of creating an interaction between the wall material and the core, and as a result, increased the efficiency of nanoencapsulation.

According to Figure 4, except for the sample containing 0.5 and 1% emulsifier under 300 bar homogenization pressure, the efficiency on day 7 of storage was higher than the first day. In other samples under different homogenization pressures, the efficiency of the nanoemulsion samples decreased on day 7 of storage.

The emulsifying properties of gum balango are related to features such as its surface activity, plasticity proper-

ties, its surface adsorption rate at the droplet surface and intramolecular interaction at the oil-water interface. In general, microencapsulated compounds remain better in emulsions with smaller particles compared to those with larger ones, and similarly, the core compounds evaporate more easily from the larger particles of the emulsion (Soottitanta-wa et al., 2005). Studies by other researchers also showed that the encapsulation efficiency increases with the decrease in emulsion particle size (Jamshidi et al. 2020; Mir-Alai Motlagh et al. 2015).

Bagheri et al. (2013) observed an encapsulation efficiency of more than 70% for encapsulation of date kernel extract with whey protein isolate. They stated that the ability of whey proteins to encapsulate polyphenols is higher than polysaccharides. Similar to these results, Faridi et al. (2015) reported an encapsulation efficiency of more than 70% for encapsulation of safranal with whey protein concentrate. Similar results have been reported for the effect of guar gum on the encapsulation efficiency of whey protein isolate (Mahyar et al., 2014) and gum arabic (Ravichandran et al., 2014) in encapsulating other bioactive compounds.

Ardestani et al. (2024) used sodium caseinate and pectin to microencapsulate crocin. According to the results of these researchers, the ratio and amount of casein and pectin used were effective on the efficiency and stability of the microcapsules.

#### Investigating the characteristics of the optimal na-

## noemulsion

According to the results obtained, the nanoemulsion containing 1% emulsifier had better efficiency and stability than other, so the stability and efficiency of this nanoemulsion at different pH, temperatures and times were investigated.

### The effect of pH on the stability and efficiency of the nanoemulsion

The effect of pH changes on the stability and efficiency of the nanoemulsion containing 1% emulsifier is shown in Table 7. There is no significant difference between the stability of the crocin nanoemulsion sample microencapsulated with sodium caseinate and balango gum at the 3 pHs studied (4, 6 and 8) ( $p > 0.05$ ), but there is a significant difference between the efficiency of the crocin nanoemulsion ( $p \leq 0.05$ ). The highest efficiency was observed at pH 4 (79%). Therefore, it can be said that pH did not affect the stability of the microencapsulated nanoemulsion, but it did affect the efficiency.

**Table 7:** Stability and efficiency of the optimal nanoemulsion under the pH changes

| pH | Stability (%)      | Efficiency (%)     |
|----|--------------------|--------------------|
| 4  | 98.33 <sup>a</sup> | 79.00 <sup>a</sup> |
| 6  | 97.00 <sup>a</sup> | 66.66 <sup>b</sup> |
| 8  | 97.66 <sup>a</sup> | 51.66 <sup>c</sup> |

\*Different lowercase letters in each column indicate significant differences ( $p \leq 0.05$ )

### 2- The effect of temperature and time on the stability and efficiency of the nanoemulsion

The effect of temperature and time on the stability and efficiency of the nanoemulsion containing 1% oleicifier is shown in Table 8.

**Table 8:** Stability and efficiency of the optimal nanoemulsion under the temperature changes

| Temperature and Time | Stability (%)       | Efficiency (%)     |
|----------------------|---------------------|--------------------|
| 65°C and 30 min      | 98.33 <sup>a</sup>  | 74.33 <sup>a</sup> |
| 80°C and 20 min      | 92.33 <sup>ab</sup> | 66.00 <sup>b</sup> |
| 95°C and 10 min      | 84.66 <sup>b</sup>  | 60.00 <sup>c</sup> |

\*Different lowercase letters in each column indicate significant differences ( $p \leq 0.05$ )

According to Table 8, with increasing temperature, the stability of the nanoemulsion and its efficiency decreased. The highest efficiency was related to the sample that was exposed to 65 ° C for 30 min (98.33%). The highest stability was related to the sample that was exposed to 65 ° C for 30 min (74.33%).

Fan et al. (2025) used whey protein isolate, chickpea and pea to microencapsulate crocin and crocein. Ac-

ording to their results, the efficiency and stability of these pigments increased with microencapsulation. In fact, hydrogen bonding interactions between protein and bioactive compounds may play a role in increasing the encapsulation efficiency and stability of microcapsules.

### Nanoemulsion properties under different drying conditions

1- Effect of inlet feed temperature and dryer air on

nanoemulsion powder particle size.

The effect of inlet feed temperature and dryer air on nanoemulsion powder particle size is given in Table 9.

**Table 9:** Particle size (nm) of nanoemulsion powder under different inlet feed and dryer air temperatures

| dryer air temp.  | 150°C                | 170°C               | 190°C               |
|------------------|----------------------|---------------------|---------------------|
| Inlet feed temp. |                      |                     |                     |
| 60°C             | 490.00 <sup>*c</sup> | 456.66 <sup>d</sup> | 406.66 <sup>e</sup> |
| 70°C             | 543.33 <sup>bc</sup> | 480.00 <sup>c</sup> | 473.33 <sup>c</sup> |
| 80°C             | 590.00 <sup>a</sup>  | 573.33 <sup>a</sup> | 526.66 <sup>b</sup> |

\*Different lowercase letters indicate significant differences ( $p \leq 0.05$ )

According to Table 9, there was a significant difference ( $p \leq 0.05$ ) between the particle size of most microencapsulated crocin nanoemulsions at different air dryer and feed temperatures. With increasing air temperature, the particle size of the microencapsulated crocin nanoemulsion decreased, and with increasing feed temperature, the particle size increased. The smallest particle size was for the nanoemulsion exposed to a dryer air temperature of 190°C and a feed temperature of 60°C (406.66 nm), and the largest particle size was for the crocin nanoemulsion exposed to an air temperature of 150°C and a feed temperature of 80°C (590 nm).

The particle size is affected by the nozzle size and position, liquid injection speed, atomizer pressure, and solution concentration (viscosity). The particle size increases with increasing viscosity and surface tension of the input liquid. Emulsion viscosity and particle size distribution have significant effects on microencapsulation in spray drying. High viscosity interferes with the atomization process and leads to the formation of large particles. With increasing temperature, viscosity and particle size should decrease; however, high temperature can cause evaporation or decomposition of some heat-sensitive compounds (Wang et al., 2009; Gharsallaoui et al., 2007). Increasing the inlet air temperature and exposing the particles to higher temperatures increases the evaporation rate, followed by swelling of the particles and the formation of a tight shell around them, which prevents the particles from shrinking during drying, leading to an increase in particle size. Previous studies have also indicated that the size of powder particles obtained from spray drying increases with increasing inlet air temper-

ature (Malekizadeh et al., 2017; Akhavan, 2006; Mahdavi et al., 2014; Aghabashlo; 2013). The effect of powder particle size on the microencapsulation efficiency of essential oils and food flavors is not clear. Some studies have indicated that larger particle sizes improve flavor retention and lower surface oil content during drying. On the other hand, no relationship was found between particle size and compound retention. Some scientists also reported that particle size alone does not affect the retention of flavor compounds and that other parameters such as emulsion particle size can have a more significant effect. Optimal particle size achieves maximum retention of volatiles. The average powder particle size retains total oil, and its minimum amount was obtained for the largest particle size. Since larger particles have a lower surface area to volume ratio, they retain better core materials. On the other hand, a longer time is required to form a layer around larger particles, and the longer the time, the greater the loss of volatiles. These two competing factors ultimately determine the degree of core material retention. Another reason for the poorer retention of volatiles in large particles may be related to the particle surface morphology (Jafari et al., 2008).

## 2- Effect of inlet feed temperature and drying air on bulk density, apparent density and porosity of nanoemulsion powder

The effect of inlet feed temperature and drying air on bulk density of nanoemulsion powder is given in Table 10. There is a significant difference ( $p < 0.05$ ) between the bulk density of most microencapsulated crocin nanoemulsions at different air drier and inlet feed temperatures. With

increasing inlet air temperature, the bulk density of microencapsulated crocin nanoemulsion increased, and with increasing inlet feed temperature, the bulk density decreased. The lowest bulk density is related to the nanoemulsion that was subjected to an air temperature of 150°C and

an inlet feed temperature of 80°C (0.50 g/cm<sup>3</sup>), and the highest bulk density is related to the crocin nanoemulsion sample that was subjected to an air temperature of 190°C and an inlet feed temperature of 60 and 70°C (0.71 g/cm<sup>3</sup>).

**Table 10:** Bulk density (g/cm<sup>3</sup>) of nanoemulsion powder under different inlet feed and dryer air temperatures

| dryer air temp.  | 150°C              | 170°C             | 190°C             |
|------------------|--------------------|-------------------|-------------------|
| Inlet feed temp. |                    |                   |                   |
| 60°C             | 0.63 <sup>*c</sup> | 0.67 <sup>b</sup> | 0.71 <sup>a</sup> |
| 70°C             | 0.54 <sup>e</sup>  | 0.61 <sup>c</sup> | 0.70 <sup>a</sup> |
| 80°C             | 0.50 <sup>f</sup>  | 0.58 <sup>d</sup> | 0.66 <sup>b</sup> |

\*Different lowercase letters indicate significant differences (p≤0.05)

According to Table 11, it is observed that with increasing dryer air temperature, the apparent density of crocin nanoemulsion increases and with increasing inlet feed temperature, the apparent density decreases. The lowest apparent density is related to the nanoemulsion that was

exposed to an air temperature of 150°C and inlet feed temperature of 80°C (1.13 g/cm<sup>3</sup>) and the highest apparent density is related to the crocin nanoemulsion sample that was exposed to an air temperature of 190°C and an inlet air temperature of 60°C (1.53 g/cm<sup>3</sup>).

**Table 11:** Apparent density (g/cm<sup>3</sup>) of nanoemulsion powder under different inlet feed and dryer air temperatures

| dryer air temp.  | 150°C                | 170°C               | 190°C               |
|------------------|----------------------|---------------------|---------------------|
| Inlet feed temp. |                      |                     |                     |
| 60°C             | 1.36 <sup>*cde</sup> | 1.40 <sup>bcd</sup> | 1.53 <sup>a</sup>   |
| 70°C             | 1.27 <sup>e</sup>    | 1.33 <sup>cde</sup> | 1.46 <sup>ab</sup>  |
| 80°C             | 1.13 <sup>f</sup>    | 1.30 <sup>de</sup>  | 1.43 <sup>abc</sup> |

\*Different lowercase letters indicate significant differences (p≤0.05)

The effect of inlet feed and dryer air temperatures

on the porosity of nanoemulsion powder is shown in Table 12.

**Table 12:** Porosity density of nanoemulsion powder under different inlet feed and dryer air temperatures

| dryer air temp.  | 150°C               | 170°C              | 190°C              |
|------------------|---------------------|--------------------|--------------------|
| Inlet feed temp. |                     |                    |                    |
| 60°C             | 0.60 <sup>*bc</sup> | 0.50 <sup>cd</sup> | 0.43 <sup>de</sup> |
| 70°C             | 0.60 <sup>bc</sup>  | 0.56 <sup>c</sup>  | 0.43 <sup>de</sup> |
| 80°C             | 0.73 <sup>a</sup>   | 0.66 <sup>ab</sup> | 0.33 <sup>f</sup>  |

\*Different lowercase letters indicate significant differences (p≤0.05)

According to the results of Table 12, the lowest porosity is related to the nanoemulsion that was subjected to an air temperature of 80 °C and an inlet air temperature of 190 °C (0.33) and the highest porosity is related to the crocin nanoemulsion sample that was subjected to a feed temperature of 80 °C and an inlet air temperature of 150 °C (0.73).

The decrease in density can be explained in terms of particle size and moisture content. With increasing temperature, the rate of moisture evaporation increases, the particle size becomes larger, and more spherical particles with less surface compaction and wrinkling are produced. Since bulk density represents the mass per unit volume of particles, the bulk density decreases with increasing particle size (Granpour et al., 2017). In the study by Sarabandi and Sadeghi Mahonak (2016), it was also pointed out that increasing particle size, increasing porosity, decreasing bulk density and bulk density of powder with increasing inlet air temperature. Density is related to particle size and its low values indicate that powders have high porosity. The advantage of powders with higher density is that large quantities can be stored in smaller containers. Higher bulk density can indicate lower amounts of air in the pores between particles, and as a result, the possibility of fat oxidation is reduced (Rodriguez-Restrepol et al., 2017; Koc and Kaymak-Ertekin, 2014). Bulk density depends on particle size, particle size distribution, particle shape, moisture, chemical composition and the amount of air trapped inside the particle. Another factor affecting bulk density is the moisture content of the powder. As the temperature increases, the moisture content decreases, the particles become lighter and as a result, the

bulk density decreases. The higher the moisture content, the greater the mass of the mass due to the presence of water and, consequently, the denser it is. In general, the effect of drying conditions on the density of the product depends largely on the type of product (Chegini et al., 2005). Porosity is inversely related to density, with low density values indicating high porosity in the powder. Porosity is an important property in the reconstitution of dried products, affecting the rehydration rate (Rodriguez-Restrepol et al., 2017; Fernandes et al., 2013). Various studies have pointed out the effect of inlet air temperature on the density and porosity of powder, and the results were consistent with the findings (Sarabandi and Sadeghi Mahonak, 2016; Akhavan Mahdavi et al., 2014; Fernandes et al., 2013; Souza et al., 2009; Jafari et al., 2008). Given that changing the feed temperature also caused a change in particle size, it also affected the density. Increasing the feed temperature, due to the reasons mentioned, caused a decrease in particle size and, as a result, an increase in bulk density. With increasing air temperature and inlet feed temperature, the trend of change in bulk density was similar to that of bulk density, but porosity had a reverse trend. Increasing air temperature usually causes a decrease in bulk density because there is a greater tendency to form porous particles (Fernandes et al., 2013).

### 3- Effect of inlet feed and drying air temperatures on moisture content and water activity of nanoemulsion powder

The effect of inlet feed and drying air temperatures on moisture content of nanoemulsion powder is given in Table 13.

**Table 13:** Moisture content (%) of nanoemulsion powder under different inlet feed and dryer air temperatures

| dryer air temp.  | 150°C              | 170°C              | 190°C             |
|------------------|--------------------|--------------------|-------------------|
| Inlet feed temP. |                    |                    |                   |
| 60°C             | 6.46 <sup>*c</sup> | 7.150 <sup>b</sup> | 7.76 <sup>a</sup> |
| 70°C             | 5.35 <sup>d</sup>  | 6.40 <sup>c</sup>  | 6.50 <sup>c</sup> |
| 80°C             | 5.13 <sup>e</sup>  | 5.56 <sup>d</sup>  | 5.63 <sup>d</sup> |

\*Different lowercase letters indicate significant differences ( $p \leq 0.05$ )

According to the results of Table 13, it is observed that with increasing air drier temperature, the moisture con-

tent of crocin nanoemulsion increased and with increasing inlet feed temperature, the moisture content decreased. The

lowest moisture content was for the nanoemulsion subjected to a feed temperature of 80°C and inlet air temperature of 150°C (5.13%) and the highest moisture content was for the crocin nanoemulsion subjected to a feed temperature of 60°C and an inlet air temperature of 190°C (7.76%).

The effect of inlet feed temperature and drying air on the water activity of the nanoemulsion powder is shown in Table 14. With increasing air drier temperature at any inlet feed temperature, the water activity of the crocin nanoemulsion increases, and at any constant air temperature, the

water activity decreases with increasing inlet feed temperature. The lowest water activity was for the nanoemulsion subjected to an inlet air temperature of 150°C and a feed temperature of 80°C (0.37) and the highest water activity was for the crocin nanoemulsion sample subjected to an inlet air temperature of 190°C and a feed temperature of 60°C (0.62). The water activity results are consistent with the moisture content results of the nanoemulsions. It is worth noting that low water activity (less than 0.6) affects the microbial and chemical stability of the final product.

**Table 14:** Water activity of nanoemulsion powder under different inlet feed temperature and dryer temperature conditions

| dryer air temp.  | 150°C              | 170°C             | 190°C             |
|------------------|--------------------|-------------------|-------------------|
| Inlet feed temp. |                    |                   |                   |
| 60°C             | 0.49 <sup>*c</sup> | 0.56 <sup>b</sup> | 0.62 <sup>a</sup> |
| 70°C             | 0.42 <sup>d</sup>  | 0.50 <sup>c</sup> | 0.57 <sup>b</sup> |
| 80°C             | 0.37 <sup>e</sup>  | 0.50 <sup>c</sup> | 0.57 <sup>b</sup> |

\*Different lowercase letters indicate significant differences ( $p \leq 0.05$ )

Increasing the temperature increases the heat transfer from the particles and causes the rate of water evaporation to increase, ultimately producing a powder with less moisture. The inlet air temperature is directly related to the drying rate and final moisture content. A low drying temperature results in the formation of particles with high-density membranes, high moisture content, low flowability, and ease of agglomeration, while a high temperature causes excess evaporation and, as a result, cracks on the particle surface. The greater the temperature difference between the particles and the drying medium, the greater the mass and energy transfer rate, and in other words, the increase in temperature acts as a driving force for the removal and removal of moisture from the particles. Accordingly, as can be seen, with an increase in the feed temperature, the temperature difference between the particles and the drying medium decreases, and as a result, moisture removal becomes more difficult and the moisture content of the powder increases. The inlet air temperature is usually determined by two factors: the temperature that can be used without damaging the product or creating operational hazards, and the comparative value of the heat source (2015; Gharsallaoui et al., 2007; Wang et al., 2008). Too high a temperature can lead to

the production of powders with high moisture content because in this case, the formation of a crust occurs very quickly, making it difficult for water to diffuse from the droplet and causing higher moisture content (Frascarlei et al., 2012). Moisture affects some powder properties such as bulk density and solubility (Peighambardest and Sarabandi, 2015). Water activity is a very important factor for spray-dried food products, affecting the shelf life of the powder. As the temperature of the drying air and the temperature difference between the air and the suspended particles increased, the water activity of the powder also decreased due to the increase in evaporation rate along with the decrease in humidity. Materials with higher water activity deteriorate faster because they have more free water available for biochemical reactions (Costa et al., 2015). Usually, foods with water activity less than 0.6 are microbiologically stable and microbial spoilage does not occur in them, but chemical reactions are possible (Peighambardest and Sarabandi, 2015).

Ghoraani et al., (2017) investigated the production of saffron bioactive compounds using microencapsulation with maltodextrin, whey protein, and gum arabic and concluded that the moisture content of microcapsules prepared with maltodextrin, whey protein, and gum arabic as wall ma-

terials varied from 31.3 to 72.5 %, which seems to be attributable to the difference in the number of water-binding groups in maltodextrin, whey protein, and gum arabic molecules. Ganji et al. (2020) used gelatin powder to microencapsulate crocin. According to their results, the moisture content of spray-dried powders increased at higher gelatin concentrations. Therefore, it can be concluded that at higher gelatin concentrations, hydrophilic protein compounds absorb more water, leading to the formation of powders with high moisture content and larger sizes. According to the results of this study, pure crocin had higher water solubility compared to encapsulated crocin at ambient temperature. In addition, the water solubility time increased significantly

at higher gelatin concentrations, which can be attributed to the difference in wall material.

#### 4- Effect of inlet feed and drying air temperatures on the efficiency of nanoemulsion powder

The effect of inlet feed and drying air temperatures on the efficiency of nanoemulsion powder is shown in Table 15. The lowest efficiency is related to the nanoemulsion that was subjected to an inlet air temperature of 150 °C and a feed temperature of 80 °C (62.80%), and the highest efficiency is related to the crocin nanoemulsion sample that was subjected to an air temperature of 190 °C and an inlet feed temperature of 60 °C (80.30%).

**Table 15:** Efficiency (%) of nanoemulsion powder under different inlet feed temperature and dryer temperature conditions

| dryer air temp.  | 150°C                | 170°C               | 190°C               |
|------------------|----------------------|---------------------|---------------------|
| Inlet feed temp. |                      |                     |                     |
| 60°C             | 76.00 <sup>*bc</sup> | 80.10 <sup>a</sup>  | 80.30 <sup>a</sup>  |
| 70°C             | 63.74 <sup>d</sup>   | 78.40 <sup>ab</sup> | 76.13 <sup>bc</sup> |
| 80°C             | 62.80 <sup>d</sup>   | 75.51 <sup>c</sup>  | 75.26 <sup>c</sup>  |

\*Different lowercase letters indicate significant differences ( $p \leq 0.05$ )

The effect of increasing temperature on the efficiency of encapsulation and release can be explained based on the change in morphology as well as the change in particle size. Higher air temperature causes shell breakage by affecting the balance between shell formation and moisture evaporation rate. In other words, higher temperatures cause faster drying of the outer surfaces than the inner surfaces and lead to the release of bioactive compounds by creating cracks in the shell (Frascarlei et al., 2012). Jafari et al. (2008) reported that in some cases, increasing the dryer air temperature by increasing the number of bubbles and surface defects causes thermal damage to the product and increases the loss during spray drying, therefore, the inlet air temperature is an important parameter in the encapsulation system.

The preservation of core materials during spray-drying coating is influenced by the composition and properties of the emulsion and the drying conditions. The short exposure time of the core material and the high rate of water evaporation keep the core temperature below 40 °C unless high temperatures are used during the process (Gharsal-

laoui et al., 2007). In some studies, the effectiveness of coating and preservation of core materials was not dependent on the inlet and outlet air temperatures in the dryer (Rojas et al., 2017). Another study found the opposite results and reported that the surface oil content decreased with increasing inlet air temperature, probably due to the high drying rate, which makes the membrane around the particle harder and therefore no more volatiles leak out (Jafari et al., 2008). Several studies have been conducted on the effect of inlet and outlet air temperatures on coating. It was shown that if the inlet air temperature is high enough (160-220 °C), it leads to the rapid formation of a semipermeable membrane on the particle surface and ensures optimal flavor retention. High air temperature causes the particle to swell due to the formation of steam inside it, resulting in thin-walled hollow particles that are unable to properly retain the core compounds (Jafari et al., 2008). Particles with a cracked shell are impermeable to gases and provide less protection for the bioactive substances inside them (Granpour et al., 2017). According to the researchers' results, the difference between the encapsulation efficiency of crocin can be due to the dif-

ference between the polymer matrices, the type of wall and the drying conditions (Ganji et al., 2020).

### 5- Effect of inlet feed and drying air temperatures on the solubility of nanoemulsion powder

The effect of inlet feed temperature and drying air on the solubility of nanoemulsion powder is shown in Table

16. With increasing air temperature at each inlet feed temperature, solubility decreased and with increasing inlet feed temperature, solubility increased. The lowest solubility was for the nanoemulsion exposed to an air temperature of 190°C and an inlet feed temperature of 60°C (80.76%) and the highest solubility was for the crocin nanoemulsion sample exposed to an inlet feed temperature of 80°C and an air temperature of 150°C (88.96%).

**Table 16:** Solubility (%) of nanoemulsion powder under different inlet feed temperature and dryer temperature conditions

| dryer air temp.  | 150°C                | 170°C               | 190°C               |
|------------------|----------------------|---------------------|---------------------|
| Inlet feed temp. |                      |                     |                     |
| 60°C             | 85.03 <sup>*bc</sup> | 83.10 <sup>cd</sup> | 80.76 <sup>e</sup>  |
| 70°C             | 85.90 <sup>bc</sup>  | 85.06 <sup>bc</sup> | 82.40 <sup>de</sup> |
| 80°C             | 88.96 <sup>a</sup>   | 86.50 <sup>ab</sup> | 85.83 <sup>bc</sup> |

\*Different lowercase letters indicate significant differences ( $p \leq 0.05$ )

Increasing the inlet feed temperature at constant air temperature increased the solubility of the powders. This is mainly due to the decrease in moisture and increase in particle size, which, according to the results of the bulk density study and the findings of the researchers, ultimately increasing the inlet feed temperature increases the porosity and improves the wettability of the particles (Peighambar-dost and Sarabandi, 2015). With increasing the dryer air temperature, the particle size increases and leads to a decrease in the time required for rehydration (Walton et al., 2000). These results are in accordance with the findings of previous studies (Costa et al., 2015; Akhavan Mahdavi et al., 2014). In some studies, it was noted that the solubility of the powder decreases with increasing the dryer temperature. With increasing temperature, due to the formation of a hard layer on the surface of the particles, the penetration of water molecules into the particle is prevented, and as a result, the solubility decreases. The effect of increasing temperature on the solubility of powders depends on the nature of the raw material, its composition and thermal sensitivity. The amount of insoluble matter formed during drying mainly depends on the protein content of the feed, the drying conditions, the temperature curve and the moisture content in the drying chamber. Product characteristics in pre-processes also play an important role in this phenomenon (Koc et al., 2010; Chegini et al., 2005). Factors such as size, shape,

composition, surface properties, particle microstructure, the presence of additives and insoluble compounds, the type of feed (solids concentration) and drying conditions (temperature used, inlet air flow rate, pressure and atomizer speed) can be very effective in the reproducibility of powders (Sarabandi and Sadeghi Mahonak, 2016).

According to the results obtained from the experiments, a spray dryer was used to dry the optimal nanoemulsion at an air temperature of 190°C and an inlet feed temperature of 60°C. The powder obtained under these conditions and drying method was subjected to the following tests.

### Release rate of crocin from an aqueous nanoemulsion containing 15% sucrose at different pH

Release at the right time and place is a very important feature in the encapsulation process that improves effectiveness, reduces the amount of additives required and increases the applicability of the compounds. The interactions that occur between the core and wall materials are among the main factors that are related to the release rate, in addition, other factors such as the volatility of the core materials, the core to wall ratio, particle size and viscosity of the wall material also affect the release (Roberts and Taylor, 2000).

The release rate of crocin from nanoemulsion in aqueous solution containing 15% sucrose at different pHs

(4, 6 and 8) at various temperatures (5, 50 and 75°C) and times (30, 60, 90, 120, 150 and 180 minutes) is shown in Figures 5, 6 and 7, respectively.

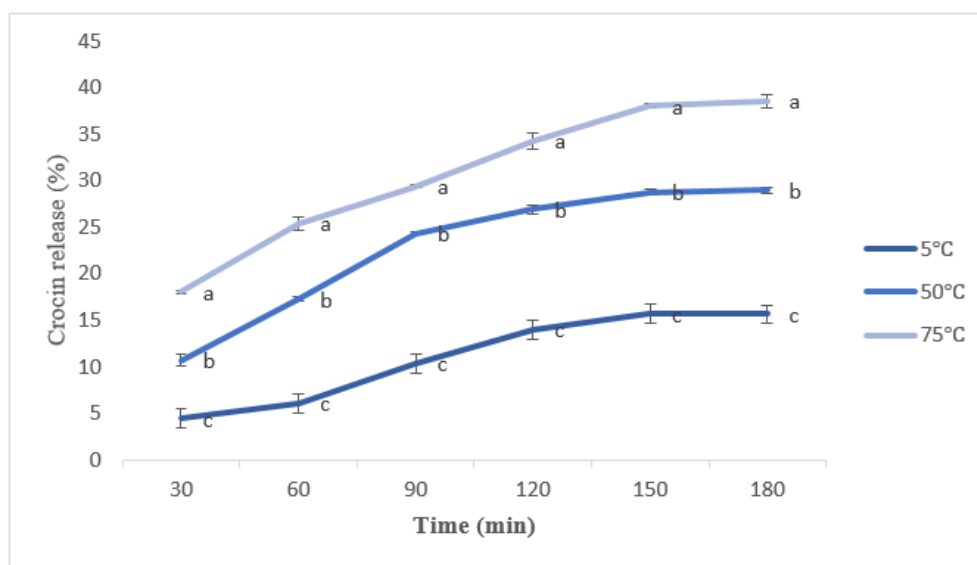


**Figure 5:** Crocin release rate at different temperatures and times at pH=4

\*Different lowercase letters indicate significant differences ( $p \leq 0.05$ )

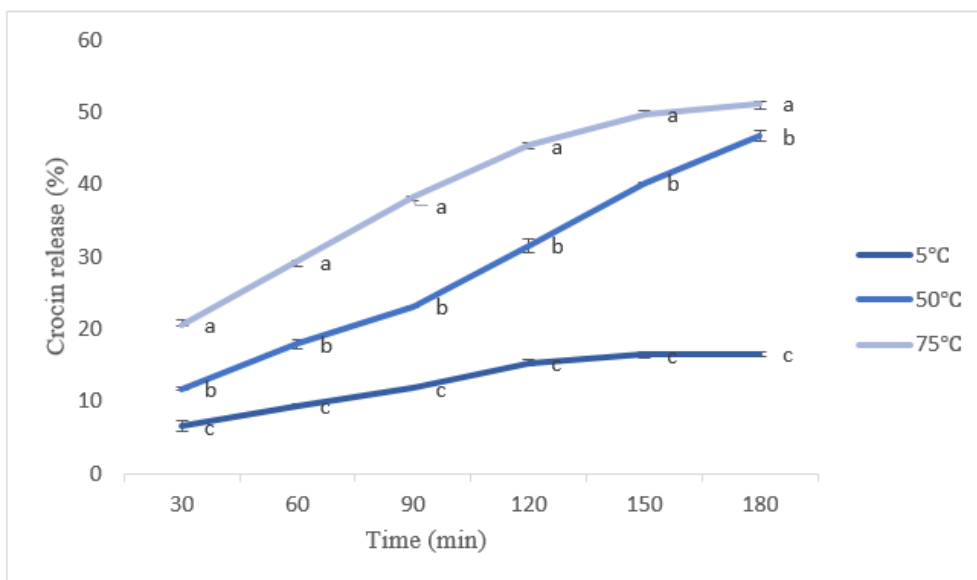


**Figure 6:** Crocin release rate at different temperatures and times at pH=6

\*Different lowercase letters indicate significant differences ( $p \leq 0.05$ )

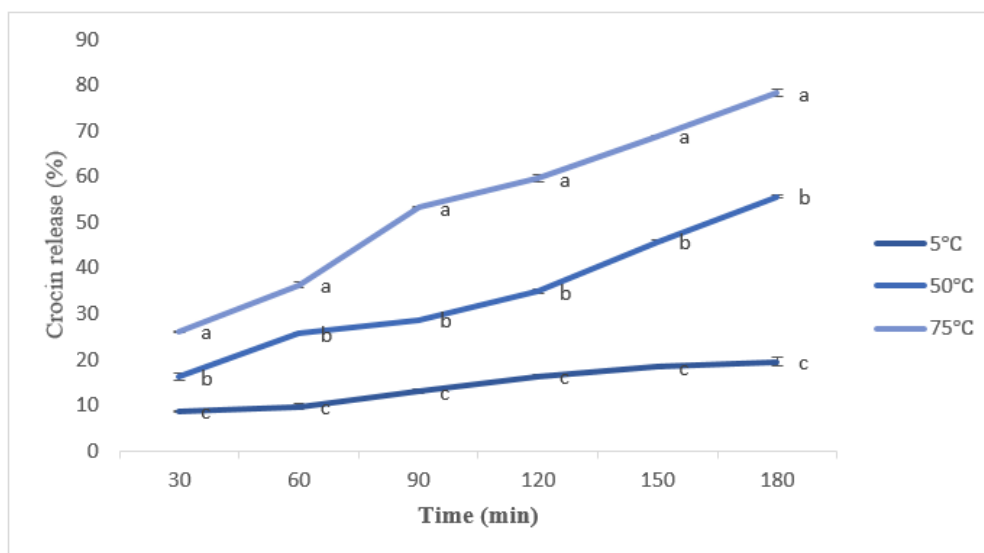


**Figure 7:** Crocin release rate at different temperatures and times at pH=8.

\*Different lowercase letters indicate significant differences ( $p \leq 0.05$ )

According to the results of Figures 5, 6 and 7, it can be seen that the rate of crocin release increased with time. Also, the rate of crocin release increased with increasing temperature, such that the highest rate of crocin release occurred at 75°C and the lowest at 5°C. The results showed that with increasing pH, the rate of crocin release increased, such that the rate of release at the temperatures studied was higher at pH 8 than the others. Therefore, the release of crocin is a function of pH, temperature and storage time. In addition, considering the results of humidity and water activity and the rate of crocin release, it can be said that these results indicated that the release depends to a large extent on the water activity of the powder and it seems that the humidity or water activity of the microcapsules determines the release rate. In addition, the release rate depends not only on temperature, but also on the relative humidity and the type of microencapsulated material. In another study, Li et al. (2011) studied the rate of carotenoid loss and adverse quality changes in saffron under different water activity and temperature conditions. They showed that the rate of carotenoid degradation and glass transition temperature of microencapsulated samples were highly sensitive to humidity and temperature, and at water activities of 0.43 to 0.53, saffron release was enhanced while the rate of carotenoid degradation remained low. In this regard, a study conducted on the release rate of limonene from powders with different walls at a temperature of 50 degrees Celsius revealed

that the rate of limonene release from microcapsules depended on the relative humidity and was intensified with its increase (Soottitantawat et al., 2005). It also seems that the increase in the release rate of saffron active ingredients after about 30 days is due to the decrease in the stability and cohesion of the biopolymers used as the coating material (wall) and the increase in the release rate under environmental stresses of temperature and humidity. One of the factors affecting mass transfer and diffusion flux is the value of the diffusion coefficient, which is directly related to temperature. The diffusion coefficient also increases with increasing temperature. Therefore, by placing the powders in an aqueous environment with a higher temperature, the rate of penetration of water molecules into them increased and water absorption and release of core materials occurred more rapidly (Salimi et al., 2018). Park and Maga (2006) reported that temperature changes can increase the release of the core. There are two different concepts in this case: temperature-sensitive release is used for materials that swell or shrink when they reach a critical temperature, and fusion-activated release, which is related to the melting of the wall with increasing temperature. As shown in the table, the release trend at low temperatures, especially 5 °C, had a low slope, while the release rate and slope of the graph increased with increasing temperature. The main mechanisms of core release are: diffusion, decomposition, use of solvent, pH, temperature and pressure. In practice, a combination of sev-

eral mechanisms is used (Desai and Park, 2005). Roointan et al. (2016) also noted that curcumin was released more at 40 ° C than at 37 ° C. pH changes can cause the release of the core material by causing changes in the solubility of the wall material. Asadpour (2016) also pointed out the increased release of folic acid encapsulated by pectin and whey protein, and attributed this to the solubility and faster decomposition of whey protein in alkaline conditions, resulting in increased release. In addition, Foegeding et al. (2002) stated that at high pH, the structure of protein molecules is more open due to increased electrostatic repulsion forces and reactivity of thiol groups. Also, in a study it was found that at high pH, the electrostatic repulsion forces within protein molecules cause their structure to open up

and increase their tendency to react with water molecules and swell, especially at highly alkaline pHs (Damodaran et al., 2008).

### Modeling the release of crocin at different temperatures in an aqueous model system containing 15% sucrose in Different pH

In order to describe the crocin release pattern, zero-order, first-order, Higuchi, Hixsoncrowell and the Peppas models were used and evaluated based on the SSE,  $r^2$  and RMSE coefficients. The results of modeling crocin release at different temperatures in the aqueous model system containing 15% sucrose at pH 4, 6 and 8 are given in Tables 17, 18 and 19, respectively.

**Table 17:** Modeling crocin release at different temperatures in the aqueous model system containing 15% sucrose (pH=4)

| Tem. (°C) | Indeces | zero-order | first-order | Higuchi | Hixson crowell | Peppas |
|-----------|---------|------------|-------------|---------|----------------|--------|
| 5         | n       | -          | -           | -       | -              | 0.771  |
|           | K       | 0.0884     | 2.887       | 0.973   | 0.913          | 0.455  |
|           | SSE     | 8.993      | 1.112       | 4.821   | 3.211          | 1.342  |
|           | $r^2$   | 0.876      | 0.984       | 0.932   | 0.914          | 0.943  |
|           | RMSE    | 1.422      | 0.523       | 9.923   | 0.978          | 0.581  |
| 50        | n       | -          | -           | -       | -              | 0.465  |
|           | K       | 0.234      | 2.25        | 2.543   | 0.982          | 3.543  |
|           | SSE     | 212.66     | 36.32       | 18.72   | 4.55           | 16.11  |
|           | $r^2$   | 0.156      | 0.654       | 0.932   | 0.884          | 0.931  |
|           | RMSE    | 6.876      | 1.932       | 91.944  | 3.761          | 1.895  |
| 75        | n       | -          | -           | -       | -              | 0.453  |
|           | K       | 0.287      | 1.889       | 3.211   | 2.916          | 4.811  |
|           | SSE     | 334.77     | 18.54       | 17.52   | 18.93          | 7.342  |
|           | $r^2$   | 0.765      | 0.942       | 0.944   | 0.965          | 0.973  |
|           | RMSE    | 8.786      | 2.081       | 1.981   | 3.546          | 1.512  |

**Table 18:** Modeling crocin release at different temperatures in the aqueous model system containing 15% sucrose (pH=6)

| Tem. (°C) | Indeces | zero-order | first-order | Higuchi | Hixson crowell | Peppas |
|-----------|---------|------------|-------------|---------|----------------|--------|
| 5         | n       | -          | -           | -       | -              | 0.546  |
|           | K       | 0.123      | 2.541       | 1.543   | 2.983          | 1.081  |

|    |       |       |       |        |        |       |
|----|-------|-------|-------|--------|--------|-------|
|    | SSE   | 37.12 | 4.652 | 4.487  | 3.821  | 2.124 |
|    | $r^2$ | 0.611 | 0.944 | 0.969  | 0.923  | 0.973 |
|    | RMSE  | 2.701 | 1.123 | 0.699  | 1.013  | 0.761 |
| 50 | n     | -     | -     | -      | -      | 0.763 |
|    | K     | 0.312 | 0.961 | 3.65   | 1.453  | 1.873 |
|    | SSE   | 63.62 | 13.21 | 104.32 | 62.124 | 13.11 |
|    | $r^2$ | 0.943 | 0.983 | 0.889  | 0.945  | 0.985 |
|    | RMSE  | 3.654 | 1.811 | 4.622  | 2.345  | 1.983 |
| 75 | n     | -     | -     | -      | -      | 0.654 |
|    | K     | 0.976 | 2.653 | 1.615  | 0.579  | 3.238 |
|    | SSE   | 28.97 | 3.112 | 6.732  | 5.723  | 10.22 |
|    | $r^2$ | 0.911 | 0.976 | 0.957  | 0.951  | 0.988 |
|    | RMSE  | 2.67  | 0.896 | 1.213  | 1.146  | 1.633 |

**Table 19:** Modeling crocin release at different temperatures in the aqueous model system containing 15% sucrose (pH=8)

| Tem. (°C) | Indeces | zero-order | first-order | Higuchi | Hixson crowell | Peppas |
|-----------|---------|------------|-------------|---------|----------------|--------|
| 5         | n       | -          | -           | -       | -              | 0.532  |
|           | K       | 0.126      | 0.12451     | 1.433   | 4.498          | 1.352  |
|           | SSE     | 17.52      | 2.645       | 1.066   | 8.543          | 0.988  |
|           | $r^2$   | 0.533      | 0.976       | 0.989   | 0.945          | 0.991  |
|           | RMSE    | 0.041      | 0.668       | 0.461   | 0.016          | 0.532  |
| 50        | n       | -          | -           | -       | -              | 0.765  |
|           | K       | 0.376      | 1.213       | 4.553   | 1.743          | 1.54   |
|           | SSE     | 8.321      | 19.52       | 112.4   | 76.132         | 14.25  |
|           | $r^2$   | 0.912      | 0.987       | 0.929   | 0.936          | 0.988  |
|           | RMSE    | 5.121      | 2.8213      | 4.86    | 3.213          | 1.897  |
| 75        | n       | -          | -           | -       | -              | 0.346  |
|           | K       | 0.532      | 1.011       | 0.976   | 2.017          | 3.762  |
|           | SSE     | 541.76     | 87.11       | 98.06   | 84.181         | 46.553 |
|           | $r^2$   | 0.764      | 0.962       | 0.958   | 0.926          | 0.977  |
|           | RMSE    | 11.23      | 5.112       | 4.564   | 3.442          | 4.112  |

The results showed that the appropriate model at pH 6 and 8 in the sucrose-containing system at all temperatures except 5°C was the Peppas model. At 5°C, the appro-

appropriate Higuchi model was determined. According to the n index in the Peppas model, the release mechanism in all cases that follow this model was combined. In other words, in

In addition to the diffusion phenomenon, the opening of polymer chains also affects the release mechanism. In an aqueous environment without sucrose, the appropriate model at pH 4 at two temperatures of 5 and 50°C was determined to be the first-order model and Peppas, respectively. The appropriate model for crocin release at different temperatures and pHs was different. At pH 4, the appropriate model, except at 5°C, was the Peppas model, while at 5°C, the appropriate model was determined to be the first-order model. In the first-order model, the rate of release of a substance from particles depends on its concentration, and the amount of substance released per unit time will always be a constant fraction of the amount of substance remaining in the system. In the Peppas relationship,  $k$  is the constant of the substance release rate, which indicates the characteristics of the carrier macromolecular network, and  $n$  is the diffusion power and represents the release mechanism (Ganjeh, 2017; Luo et al., 2011). The Peppas model considers the substance release mechanism as a combination of simple diffusion (Fick's law) and type II transport (diffusion of water into the carrier network and its swelling). In all pHs studied, the value of  $n$  was less than 1.

Nazari et al. (2023) investigated the release rate of crocin microencapsulated with soy protein concentrate, pectin, and gum arabic. According to their results, the highest release of crocin was related to crocin microencapsulated with soy protein concentrate, and the lowest was related to crocin containing pectin. It seems that the macromolecule pectin is a factor in preventing its release. Mohammadi et al. (2016) produced double emulsions using whey powder and pectin and showed that adding pectin to the external aqueous phase and complexing it with whey powder reduced the release of phenolic compounds. The release methods of compounds from polymer networks include diffusion, swelling of the polymer network, and degradation of biopolymer materials. Since biopolymers are pre-hydrated, the release mechanism in double emulsions is diffusion. Breakage due to strong shear force or due to swelling of in-

ternal water droplets may lead to rupture, and diffusion through narrow channels is possible. The release component depends on the geometric shape of the drug structure and the physical mechanism of release (Nazari et al., 2023).

Ardestani et al. (2024) used sodium caseinate and pectin to microencapsulate crocin. According to these researchers, rheological findings showed that shear thinning behavior in microcapsules with crosslinking had little effect on the interconnected elastic gel structures. However, crosslinking improved the thermal and structural properties of the microcapsules. Increasing the polymer chain length due to crosslinking and the presence of a guest molecule (saffron extract) resulted in higher rheological moduli, indicating increased entanglements and good correlation with the thermal, structural and microstructural properties of the coacervates. Crocin release rate and release modeling from nanoemulsion powder in a simulated gastrointestinal system over the past few decades, there has been great progress in the field of controlled release of bioactive substances from nano- and microcarriers. Release patterns can be slow or rapid initial release followed by a sustained release. The aim of controlled release systems is to maintain the concentration of the bioactive agent at an appropriate level. In other words, these systems are able to control the rate and duration of release of the active agent. For this purpose, the use of mathematical models is very useful and allows the prediction of release kinetics. Also, in most cases, it is possible to measure some important physical parameters such as the diffusion coefficient of the active agent and reach a suitable model with the experimental data obtained. Therefore, mathematical modeling is of great value in optimizing the formulation process (Dash et al., 2010).

### **The percentage of crocin release from the nanoemulsion in the simulated stomach and intestine system**

At different times is shown in Figure 8 and the modeling of crocin release under simulated stomach and intestine conditions is shown in Table 20.

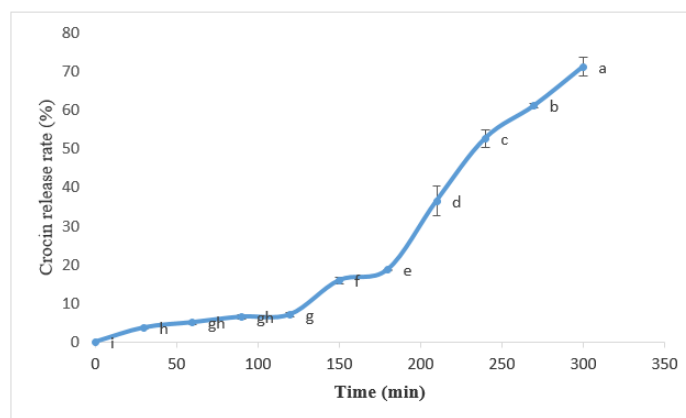


**Figure 8:** Crocin release rate from nanoemulsion powder in simulated stomach and intestine system

According to Figure 8, with increasing time, the release rate of crocin in the simulated stomach system increases. It should be noted that the pH of the stomach is acidic.

**Table 20:** Modeling of crocin release in simulated stomach and intestine conditions

| Emulsion powder. (g) | Indeces | zero-order | first-order | Higuchi | Hixson crowell | Peppas |
|----------------------|---------|------------|-------------|---------|----------------|--------|
|                      | n       | -          | -           | -       | -              | 1.88   |
|                      | K       | 0.321      | 10.35       | 2.867   | 0.165          | 0.011  |
| 0.5                  | SSE     | 1124       | 1655        | 3011    | 777            | 124    |
|                      | $r^2$   | 0.876      | 0.877       | 0.678   | 0.912          | 0.987  |
|                      | RMSE    | 10.12      | 41.15       | 16.89   | 8.765          | 4.876  |
|                      | n       | -          | -           | -       | -              | 2.011  |
|                      | K       | 0.234      | 10.55       | 2.865   | 0.564          | 124.87 |
| 1                    | SSE     | 987.66     | 1621        | 2786    | 776.89         | 14.25  |
|                      | $r^2$   | 0.867      | 0.711       | 0.687   | 0.912          | 0.981  |
|                      | RMSE    | 10.111     | 38.12       | 17.23   | 8.342          | 3.641  |

According to the correlation coefficient obtained for acidic conditions of the stomach, the Peppas model was defined as the best model. The mechanism of crocin release was determined by the Peppas model. In this model, the n parameter determines the release mechanism. Based on the results of the research of Kavousi (2016), for  $n < 0.5$ , the release occurs through the diffusion mechanism, for  $n < 1.0 > 0.5$  through the erosion and diffusion mechanism, and for  $n > 1$ , through the erosion mechanism. According to the data obtained, it can be concluded that the mechanism of crocin release in the stomach environment and the concentration of 0.5 and 1% of the microencapsulated powder

was probably through the erosion mechanism. In the research of Kavousi (2016), the best release model in gastric conditions was the Ritger-peppas model with the diffusion mechanism, and in intestinal conditions, the Peppas model with the erosion mechanism. Delphia and Thangavel (2017) reported that the best release model for microencapsulated curcumin in egg albumin and dried by spray drying was the Hixson-crowell model, followed by the first-order model under intestinal conditions after 72 hours.

Nazari et al. (2023), in their study of crocin microencapsulated with soy protein concentrate, gum arabic and pectin, showed that the best model to explain the re-

lease behavior of crocin in the stomach was the Ritger-peppas model, followed by the zero-order model. The best model in the intestine was the Peppas model and the first-order model in general. The high release rate in the stomach indicated that initially, due to the high concentration gradient of crocin, the release of this bioactive compound was time-independent and approached a linear model.

Saroglu et al. (2021) stated that encapsulation prevents the degradation of these compounds by environmental factors, degradation in the human digestive tract and provides controlled release of the compounds, thereby improving bioavailability. Ardestani et al. (2024) used sodium caseinate and pectin to microencapsulate crocin. According to the results of these researchers, release kinetic studies showed a slower release in the gastric phase compared to the intestinal phase, and the Ritger-peppas model effectively described the release of saffron extract and highlighted the dominant release mechanism of swelling and dissolution. Therefore, the wall materials of crocin caused the stability of saffron in the gastric phase and its sustained release. In the intestinal phase, it enhances the excellent absorption of saffron in simulated digestion.

## Conclusions

In general, the results showed that the largest particle size was for the sample containing 0.25% emulsifier under 500 bar pressure and the smallest particle size was for the sample containing 1% emulsifier under 500 bar pressure. In the coated nanoemulsion samples with 0.5 and 1% emulsifier, the efficiency increased with increasing emulsifier content and homogenization pressure. The highest efficiency was observed at pH 4. With increasing temperature, the stability of the nanoemulsion and its efficiency decreased. The highest efficiency was for the sample that was exposed to 65°C for 30 minutes. With increasing inlet feed

temperature, the particle size of the coated crocin nanoemulsion increased. With increasing air temperature at each inlet feed temperature, the bulk density of crocin nanoemulsion decreased, and the highest porosity was found in the crocin nanoemulsion sample that was exposed to a feed temperature of 80°C and an inlet air temperature of 150°C. Over time, the crocin release rate increased. At all pHs studied, the crocin release rate increased with increasing temperature, such that the highest crocin release rate occurred at 75°C and the lowest at 5°C. In the sucrose-containing system at pH 4, the appropriate model was the Peppas model, except at 5°C, while at 5°C, the appropriate model was the first-order model. Finally, the results showed that crocin-containing nanocapsules stabilized this pigment in the simulated stomach and intestine.

## Conflict of interest

The authors declare no competing interest.

## Funding

Not applicable.

## Author's contribution statement

**R.E.** was responsible for conceiving and designing the experiments, laying the groundwork for the study. **L.R.** and **S.J.** took on the hands-on task of performing the experiments, ensuring their execution according to the design. The data analysis was carried out by **L.R.**, who delved into the results and extracted meaningful insights. The writing and proofreading of the final paper were undertaken by **F.S.** and **M.D.** All authors reviewed the completed manuscript and gave their consent for its publication, signifying their agreement with the content and findings reported in the study. All authors reviewed the manuscript.

## References

1. Acosta, E. 2009. Bioavailability of nanoparticles in nutrient and nutraceutical delivery. *Current Opinion in Colloid and Interface Science*. 14(1): 3-15.
2. Akhavan Mahdavi, S., Jafari, S. M., Ghorbani, M. and Assadpoor, E. 2014. Spray-drying microencapsulation of anthocyanins by natural biopolymers: a review. *Drying Technology*. 32: 509–518.
3. Alouk, I., Lv, W., Chen, W., Miao, S., Chen, C., Wang, Y., & Xu, D. (2025). Encapsulation of *Monascus* pigments in gel in oil in water (G/O/W) double emulsion system based on sodium caseinate and guar gum. *International Journal of Biological Macromolecules*, 285, 138232.
4. An Y, Yan X, Li B, Li Y. Microencapsulation of capsanthin by self-emulsifying nanoemulsions and stability evaluation. *European Food Research and Technology*. 2014; 239(6):1077–85.
5. Ardestani, F., Haghighi Asl, A., & Rafe, A. (2024). Characterization of caseinate-pectin complex coacervates as a carrier for delivery and controlled-release of saffron extract. *Chemical and Biological Technologies in Agriculture*, 11(1), 118.
6. Bagheri L, Madadlou A, Yarmand M, and Mousavi ME, 2013. Nanoencapsulation of date palm pit extract in whey protein particles generated via the desolvation method. *Food Research International* 51: 866-871.
7. Chegini, G. R. and Ghobadian, B. 2005. Effect of spray-drying conditions on physical properties of orange juice powder. *Drying Technology*. 23: 657-668.
8. Chen, B., Li, H., Ding, Y. and Suo, H. 2012. Formation and microstructural characterization of whey protein isolate/beet pectin coacervations by laccase catalyzed cross-linking. *LWT- Food Science and Technology*. 47 (1): 31-38.
9. Costa, S. S., Machado, B. A. S., Martin, A. R., Zagnara, F., Ragadalli, S. A. and Alves, A. R. C. 2015. Drying by spray drying in the food industry: Micro-encapsulation, process parameters and main carriers used. *African Journal of Food Science*. 9 (9): 462-470.
10. Damodaran, S., Parkin, K. L. and Fennema, O. R. 2008. *Fennema's Food Chemistry*. CRC Press, Taylor and Francis Gp, Boca Raton.
11. Dash, S., P. N. Murthy, L. Nath and P. Chowdhury. 2010. Kinetic modeling on drug release from controlled drug delivery systems. *Acta Poloniae Pharmaceutica*. 67(3): 217-223.
12. Desai, K. G. H. and Park, H. J. 2005. Recent developments in microencapsulation of food ingredients. *Drying Technology*. 23 (7): 1361-1394.
13. Dickinson E, 2003. Hydrocolloids at interfaces and the influence on the properties of dispersed systems. *Food Hydrocolloids* 17:25–39.
14. Fan, W., Shi, Y., Hu, Y., Wang, S., Zhang, J., & Liu, W. (2025). Construction of W/O/W microcapsules based on the combination of polyglycerol polyricinoleate/protein for the co-encapsulation of crocin and quercetin: Physical properties, stability and in vitro digestion. *Food Chemistry*, 473, 142985.
15. Fang, Z., and Bhandari, B. 2010. Encapsulation of polyphenols—a review. *Trends in Food Science & Technology*. 21(10): 510-523.
16. Faridi Esfanjani A, Jafari SM, Assadpoor E, Mohammadi A, 2015. Nano-encapsulation of saffron extract through double-layered multiple emulsions of pectin and whey protein concentrate. *Journal of Food Engineering* 165: 149-155.
17. Fernandes, R. V. B., Borges, S. V. and Botrel, D. A. 2013. Influence of spray drying operating conditions on microencapsulated rosemary essential oil properties. *Ciência e Tecnologia de Alimentos*. 33 (1): 171-178.
18. Foegeding, E. A., Davis, J. P., Doucet, D. and McGuffey, M. K. 2002. Advances in modifying and understanding whey protein functionality. *Food Science and Technology*. 13: 151-159.
19. Frascareli, E. C., Silvaa, V. M., Tonona, R. V. and Hubingera, M. D. 2012. Effect of process conditions on the microencapsulation of coffee oil by spray drying. *Food and Bioproducts Processing*. 90: 413-424.

20. Ghasemi, S., Jafari, S. M., Assadpour, E. and Khomeiri, M. 2017a. Production of pectin- whey protein nano-complexes as carriers of orange peel oil. *Carbohydrate Polymers*. 177: 369-377.
21. Gharsallaoui, A., Roudaut, G. L., Chambin, O., Voille, A. and Saurel, R. 2007. Applications of spray-drying in microencapsulation of food ingredients: An overview. *Food Research International*. 40: 1107-1121.
22. Guimaraesr Sousa MJ, Carvalho AM and Ferreira ICFR, 2010. Targeting excessive free radicals with peels and juices of citrus fruits: Grapefruit, Lemon, Lime and Orange. *Journal of Food and Chemical Toxicology*, 48: 99-106.
23. Harte, F. and Venegas, R. 2010. A model for viscosity reduction in polysaccharides subjected to high pressure homogenization. *Journal of Texture Studies*. 41 (1): 49-61.
24. Hasani, F., Pezeshki, A. and Hamishehkar, H. 2015. Effect of surfactant and oil type on size droplets of beta-carotene-bearing nanoemulsions. *International Journal of .Current Microbiology and Applied Science*. 4 (9): 146-155.
25. Jafari, S. M., Assadpoor, E., He, Y. and Bhandari, B. 2008a. Encapsulation efficiency of food flavours and oils during spray drying. *Drying Technology*. 26: 816-835.
26. Jafari, S. M., Assadpoor, E., He, Y. and Bhandari, B. 2008b. Re-coalescence of emulsion droplets during high-energy emulsification. *Food Hydrocolloids*. 22 (7): 1191-1202.
27. Jamshidi M, Esmailzadeh Kenari R, Motamedzadegan A and Biparava P, 2020. Encapsulation of Unsaponifiable Matter of Rice Bran Oil Bychitosan and *Lepidium perfoliatum* Seed Gum: Characterization and Antioxidant Activity, *Journal of the American Oil Chemists' Society* 7(21):1-9.
28. Juttulapa, M., Piriyaarasarth, S., Takeuchi, H. and Sriamornsak, P. 2017. Effect of high-pressure homogenization on stability of emulsions containing zein and pectin. *Asian Journal of Pharmaceutical Sciences*. 12: 21-27.
29. Karadag, A., Yang, X., Ozcelik, B. and Huang, Q. 2013. Optimization of preparation conditions for quercetin nanoemulsions using response surface methodology. *Journal of Agricultural and Food Chemistry*. 61: 2130-2139.
30. Kharat, M., Zhang, G. and McClements, D. J. 2018. Stability of curcumin in oil-in-water emulsions: Impact of emulsifier type and concentration on chemical degradation. *Food Research International*. 111: 178-186.
31. Koç, B. and Kaymak-Ertekin, F. 2014. The effect of spray drying processing conditions on physical properties of spray dried maltodextrin. *Foodbalt*. 17: 243-247.
32. Koc, B., Yilmazer, M. S, Balkır, P. and Ertekin, F. K. 2010. Spray drying of yogurt: optimization of process conditions for improving viability and other quality attributes. *Drying Technology*. 28: 495-507.
33. Li, N., Taylor, L.S., and Mauer, L.J. 2011. Degradation kinetics of catechins in green tea for pigments and flavors with solvents, centrifuging and mixing to form solutions. (U.S. Pat.7, 070,823).
34. Luo, Y., Zhang, B., Whent, M., Yu, L. and Wang, Q. 2011. Preparation and characterization of zein/chitosan complex for encapsulation of  $\alpha$ -tocopherol, and its in vitro controlled release study. *Colloids and Surfaces Biointerfaces*. 85: 145-152.
35. McClements, D. J. 2015. Encapsulation, protection and release of hydrophilic active components: Potential and limitations of colloidal delivery systems. *Advances in Colloid and Interface Science*. 219: 27-53.
36. Mohammadi A, Jafari SM, Assadpour E, Faridi Esfajani A. Nano-encapsulation of olive leaf phenolic compounds through WPC-pectin complexes and evaluating their release rate. *Int J Biol Macromol*. 2016; 82:816–22.
37. Najafi, M.N., Kadkhodae, R., and Mortazavi, S.A. 2011. Effect of drying process and wall material on the properties of encapsulated cardamom oil. *Food biophysics*, 6(1): 68-76.
38. Nazari, Z., & Asili, J. (2023). Nanoencapsulation of crocin in double-layer emulsions for improved stability and enhanced efficacy against depression. *Plos one*, 18(10), e0289425.
39. Park, D. and Maga, J. A. 2006. Identification of key volatiles responsible for odour quality differences in popped popcorn of selected hybrids. *Food Chemistry*. 99 (3):

538-545.

40. Pedras, M. M., Pinho, C. R. G., Tribst, A. A. L., Franchi, M. A. and Cristianini, M. 2012. The effect of high pressure homogenization on microorganisms in milk. *International Food Research Journal*. 19 (1): 1-5.
41. Ravichandran K, Palaniraj R, Saw NMT, Gabr AMM, Ahmed AR, Knorr D and Smetanska I, 2014. Effects of different encapsulation agents and drying process on stability of betalains extract. *Journal of Food Science and Technology* 51(9): 2216-2221.
42. Saroglu, O., Bekiroglu, H., & Karadag, A. (2021). Encapsulation of saffron bioactive compounds. In *Saffron* (pp. 183-220). Academic Press.
43. Rodríguez-Restrepo, Y. A., Giraldo, G. H. and Rodríguez-Barona, S. 2017. Solubility as a fundamental variable in the characterization of wall material by spray drying of food components: Application to microencapsulation of *Bifidobacterium animalis* subsp. *Lactis*. *Journal of Food Process Engineering*. 15: 1-8.
44. Rojas-Moreno<sup>1</sup>, S., Cardenas-Bailon, F., Osorio-Revilla, G., Gallardo-Velazquez, T. and Proal-Najera, J. 2017. Effects of complex coacervation-spray drying and conventional spray drying on the quality of microencapsulated orange essential oil. *Journal of Food Measurement and Characterization*. doi.org/10.1007/s11694-017-9678-z.
45. Roointan, M., Sharifi-Rad, F. and Badrzadeh, J. and Sharifi-Rad. 2016. comparison between PLGA-PEG and NI-PAAm-MAA nanocarriers in curcumin delivery for hTERT silencing in lung cancer cell line. *Cellular and molecular biology*. 62: 51-56.
46. Soottitantawata A, Bigeardb F, Yoshiia H, Furutaa T, Ohkawarac M and Linkod P, 2005. Microencapsulation of l-menthol by spray drying and its release characteristics. *Innovative Food Science and Emerging Technologies* 6:107–114.
47. Souza, A. S., Borges, S. V., Magalhaes, N. F., Ricaco, H. V., Cereda, M. P. and Dauto, E. R. 2009. Influence of spray drying conditions on the physical properties of dried pulp tomato. *Ciência e Tecnologia de Alimentos*. 29 (2): 291-294.
48. Taherian AR, Fustier P, Ramaswamy HS. Effect of added oil and modified starch on rheological properties, droplet size distribution, opacity and stability of beverage cloud emulsions. *J. Food Eng.* 2006; 77(3): 687-96.
49. Walton, D. E. 2000. The morphology of spray-dried particles. A qualitative view. *Drying Technology*. 18: 1943-1986.
50. Wang, X., Jiang, Y., Wang, Y.Y., Huang, M., Hoa, C. and Huang, Q. 2008. Enhancing anti-inflammation activity of curcumin through O/W nanoemulsions. *Food Chemistry*. 108: 419-424.
51. Wang, Y., Lu, Z., Lv, F. and Bie, X. 2009. Study on microencapsulation of curcumin pigments by spray drying. *European Food Research Technology*. 229: 391-396.
52. Wang Y, Li D, Wang L, Adhikari B. The effect of addition of flaxseed gum on the emulsion properties of soybean protein isolate (SPI). *J Food Eng.* 2011; 104(1): 56-62.
53. Yang Y, Marshall-Breton C, Leser ME, Sher AA, McClements DJ. Fabrication of ultrafine edible emulsions. Comparison of high-energy and low-energy homogenization methods. *Food Hydrocolloids*. 2012; 29(2):398–406.
54. Yong, A. P., Aminul Islam, M. D. and Hasan, N. 2017. The effect of pH and high-pressure homogenization on droplet size. *International Journal of Engineering Materials and Manufacture*. 2 (4): 110-122.
55. Peighamardoust S.H. and Sarabandi Kh. 2015. Effect of spray drying conditions on the physicochemical properties, production yield of malt extract powder. *Journal of Food Industry Research*. 25 (2): 314-299.
56. Sarabandi, K. and Sadeghi Mahonak, A. 2016. The effect of inlet air temperature and maltodextrin content on the physical and chemical properties of spray-dried date juice powder. *Journal of New Food Technologies*. 4 (14): 1-15.
57. Qurani B. Kadkhodaei R. Al-Hosseini A. The effect of biopolymer type, temperature and relative humidity on the physicochemical properties and stability of microencapsulated saffron bioactive compounds.
58. Ghanbarzadeh B, Almasi D, Niknia N, 2013, Chem-

istry and Physics of Colloidal Systems and Food Biopolymer Solutions, Sharif University of Technology Publications.

59. Ganjah, M. 2017. Nanoencapsulation of limonene by starch nanoparticles and modeling its release in simulated systems and model beverage formulation. PhD thesis. Gorgan University of Agricultural Sciences and Natural Resources,

Gorgan.

60. Malekizadeh, N., Peighambaroust, S. H., Olad Ghafari, A. and Sarabandi, K. 2018. The effect of different concentrations of maltodextrin and different spray drying temperatures on the properties of microencapsulated sumac extract powder. Journal of Research on Food Sciences and Industries of Iran. 14 (2): 334-321.

### Submit your manuscript to a JScholar journal and benefit from:

- ☞ Convenient online submission
- ☞ Rigorous peer review
- ☞ Immediate publication on acceptance
- ☞ Open access: articles freely available online
- ☞ High visibility within the field
- ☞ Better discount for your subsequent articles

Submit your manuscript at  
<http://www.jscholaronline.org/submit-manuscript.php>